THE ROLE OF CAPILLARIES IN THE PATHOGENESIS OF DELAYED RADIONECROSIS OF BRAIN

LARRY W. McDONALD, M.D., AND THOMAS L. HAYES, PH.D.

From The Division of Medical Physics, Donner Laboratory and Lawrence Radiation Laboratory, University of California, Berkeley, Calif.

Necrosis appearing in tissue of the central nervous system months or even years after local exposure of the tissue to ionizing radiation is a limiting factor in radiation therapy when either the brain or spinal cord must be included in the radiation field.[1-3] Many authors have stressed the importance of blood vessels in the pathogenesis of late radionecrosis of brain and spinal cord because of the marked sclerosis of small arteries that one sees about areas of delayed radionecrosis.[4,5] Some have attributed the lesion partly to vascular effects, but much more to differential effects on various cellular elements in the area of injury.[6] Others have studied the lesion during its early development and, using nucleosides labeled with tritium, have noted increased labeling of glial cells and increased numbers of glial cells immediately preceding the appearance of the necrosis.[7]

Since sclerosis of blood vessels is usually not observed with the light microscope prior to the appearance of distinct necrosis, it has often been considered secondary to the general tissue breakdown and not a primary cause of the necrosis. When it occurs, necrosis involves most cellular components, and for this reason failure of the vascular supply would explain the lesion. Because the structures of the capillary wall are at the limits of resolution of the light microscope, alterations in these vessels produced by radiation and preceding or accompanying radionecrosis have not been given attention. The present study was undertaken to determine if alterations in the capillary could be found with the electron microscope to precede or occur concomitantly with the tissue necrosis.

MATERIALS AND METHODS

Twenty-two male New Zealand White rabbits were used in the study. The ages of the animals at the time of irradiation and post-irradiation intervals to the time of sacrifice are given in Tables I, II, III, IV, and V. In order to insure well-localized radiation, the cyclotron-produced particle beams were used throughout.[8-11] The

Supported by the U. S. Atomic Energy Commission.

Presented in part at the 54th Annual Meeting of the International Academy of Pathology, Philadelphia, Pa., 1965.

Accepted for publication Nov. 11, 1966.

sensory cortex was irradiated using radiographs of the head to position the beam (Fig. 1). When the proton beam was used, the beam was directed dorsoventrally; the range of this beam was 1.3 to 1.6 cm. When the alpha-particle beam was used, it was directed transversely through the same area of cerebral cortex. The range of this beam is more than 20 cm., so that it passed through the head and out the other side. All doses were given as single exposures with dose rates of 500 to 1000 rad/min. for the alpha particles and 10,000 to 30,000 rad/min. for the protons. Most animals were injected intravenously with 1 ml. of 10% trypan blue solution the day preceding sacrifice to help identify the irradiated area. All animals were perfused through the ascending aorta with 5% glutaraldehyde in 0.1 M phosphate buffer while under pentobarbital anesthesia. Some animals were premedicated with chlorpromazine. A perfusion pressure of 3 ft. of water was used. Heparin solution (0.5 cc. of a 1:1000 dilution) and 0.5 cc. of 2% $NaNO_2$ solution were injected into the left ventricle immediately prior to inserting the cannula into the ascending aorta to start the perfusion. The blood was flushed from the vascular bed with about 150 ml. of Palay's [12] balanced salt solution at room temperature until the flow from the incised right atrium began to clear. Then the glutaraldehyde at 4° C. was started and run at a rate of 800 ml. in 45 min.

After completion of the perfusion the brain was cut transversely through the irradiated area, half of the irradiated area being taken for light microscopy and the other half being used for electron microscopy. All tissue for light microscopy was stained with hematoxylin and eosin and luxol fast blue. In addition, many tissue sections were stained with cresyl violet, phosphotungstic acid hematoxylin (PTAH), periodic acid-Schiff (PAS), or Holmes' silver stain for nerve fibers. Tissue for electron microscopy was handled in 2 ways. In all animals except Rabbits 5, 6, 7, 8, 9, and 25 (Tables II and V), tissue from the presumed irradiated area and control tissue from at least 1 cm. anterior to the irradiated area was minced in Palade's fixative at 4° C. Fixation was then continued in Palade's fixative for 1 hr. Then the tissue was dehydrated in graded alcohols and embedded in Araldite according to the procedure of Glauret [13] or in Epon 812 using the procedure of Luft.[14] Sections were cut on a Sorvall MT-2 ultramicrotome using glass knives and stained on the grids with uranyl acetate and Reynold's [15] lead citrate solution. Specimens were examined and photographed using an Hitachi HU-11 electron microscope. Basal lamina thickness measurements were made from one outermost border to the other.

In order to examine specifically areas of early necrosis measuring less than a few hundred micra in diameter, a large-block embedding and recovery procedure was developed so that the local areas of radionecrosis could first be found with the light microscope and then taken for examination in the electron microscope. We have also used this procedure successfully to isolate microscopic areas in skin and bone marrow for electron microscopy. The procedure was used for Rabbits 5, 6, 7, 8, and 9, as indicated in Table II, and for Rabbit 25, as indicated in Table V. This technique consists of taking a block of tissue from the presumed irradiated area after completion of the glutaraldehyde perfusion as described above. This block of tissue, 4 mm. in thickness and generally consisting of the entire cross section of 1 cerebral hemisphere, is placed in a 40% solution of OsO_4 in carbon tetrachloride at 4° C. for 1 hr., following which dehydration and embedding in Epon 812 are done according to the following schedule:

1. 70%, 80%, and 95% ethanol, 30 min. each.
2. 100% ethanol, 3 changes, 1 hr. in each.
3. Propylene oxide, 3 changes, 1 hr. in each.
4. Epon 812, 2 hr. in partial vacuum or overnight.
5. Epon 812, 12 hr. in partial vacuum.
6. Epon 812, 24 hr. in partial vacuum.
7. Embed in Epon 812 with 0.015 parts of DMP-30 added.

The tissues in the embedding molds are kept at room temperature and atmospheric pressure for 24 hr., following which they are transferred to a 55–60° C. oven until polymerization is complete (about 72 hr.). All Epon mixtures, made according to Luft,[14] are used with an A to B ratio of 1 to 1. The vacuum used is adjusted to a predetermined gauge reading such that bubbles will not quite appear in the plastic. After completion of the polymerization, sections are cut at 4 μ using a heavy sledge microtome, the Jung Model K microtome, and a No. K-2 knife. These sections may be collected dry with a brush or with a brush dipped in 70% alcohol and mounted on slides by floating on an absolute alcohol bath. After taking the sections to xylene, cover slips are applied with Permount. The sections can be examined unstained or they may be stained with a stock Giemsa solution for 30 min. After examining the mounted sections and finding the desired area for electron microscopy, the slide is matched to the cut tissue-block face under the dissecting microscope and the desired area is removed from the block in a 0.5-mm. cube with a pointed Bard-Parker (No. 11) scalpel blade. This small 0.5-mm. block is then placed in 1 part propylene oxide and 1 part of Epon 812. After 30 min. it is transferred to pure Epon with 1.5% DMP-30 in the capsules. After polymerization for 48 hr. at 60° C. the ultrathin sections are cut and stained with uranyl acetate and Reynold's lead citrate,[15] and examined in the electron microscope as above.

Since the initiation of this work, Grimley [16] has independently developed a similar technique. He, however, does not use tissue blocks as thick as those that can be examined by the method described here. This is because the 40% OsO_4 employed in our method has double the penetration of a 1% aqueous solution, and thus allows the use of thicker blocks. Grimley [16] also re-embeds the tissue from the light-microscopy section for ultrathin sectioning for electron microscopy. We have tried this since the appearance of his paper, but find some difficulty with fracturing of the tissue when it is removed from the section for electron microscopy as he described. In the technique developed by De Bruijn and McGee-Russell,[17] which has similarities to both our technique and that of Grimley,[16] one cuts out the selected area from the large block for ultrathin sectioning using a small trephine or one grinds down the block face around the selected area with a dental bur.

In order to confirm capillary changes in areas adjacent to necrotic tissue, we have used the scanning electron microscope.[18] We have developed a technique for examining standard-size light-microscopy sections with this instrument. The details of this technique are the subject of another paper.[19] Secondary electrons were used to build up the scanning microscope image.

To evaluate capillary alterations further, focal necrosis was produced in the right cerebrum of one rabbit by injecting a 2% suspension of glass beads 14–40 μ in diameter into the right internal carotid artery. Two weeks following the injection, the animal was sacrificed and examined by conventional light microscopy with the stains already described. In addition, large blocks were embedded in Epon 812, and areas adjacent to necrotic foci were taken for transmission electron microscopy using the large-block recovery method.

Results

Microscopic changes are recorded in Tables I, II, III, IV, and V. In the proton-irradiated brains, the area at the end of the beam path (Bragg peak) was not studied because the effective radiation dose (as compared to conventional X-ray) [9] is higher there than indicated in the tables. With doses greater than 20 krad (Table I), a radiation-induced hole in the sensory cortex is usually seen (Fig. 1). This lesion has a "punched-out" appearance and on light microscopy it is found to have a narrow

TABLE I

RESULTS WITH PROTON IRRADIATION USING DOSES GREATER THAN 20 KRAD AND AN APERTURE OF ONE-EIGHTH IN.

Rabbit No.	*Area tissue studied*	*Dose (krad)*	*Energy (mev)*	*Age at irrad. (days)*	*Days aft. irrad. at sacrifice*	*Gross les.*	*Microscopic findings **						
							Light microscopy			*Electron microscopy*			
							Hemorrhage	*Gliosis*	*Demyelination*	*Capil. basal lamina thick.†*	*Incr. fibrils in foot processes*	*Endothel. swell.*	*Capil. stasis*
1	Irrad.‡	26.6	37.5	54	33	+	NE	NE	NE	110/4	+++	+++	+++
	Control	0	—	—	—	0	0	0	0	85/4	0	0	0
2	Irrad.	20.6	42.0	56	67	+	0	+++	++	NE	NE	NE	NE
	Control	0	—	—	—	0	0	+	0	NE	NE	NE	NE
3	Irrad.	25.0	37.5	86	69	+	0	++	+	NE	NE	NE	NE
	Control	0	—	—	—	0	0	0	0	67/6	0	+	+
4	Irrad.	26.3	37.5	84	69	0	+	+++	++	185/5	+++	++	+
	Control	0	—	—	—	0	0	0	0	66/5	0	0	+

* NE, not examined.

† Expressed as average thickness in millimicrons per number of measurements on different capillaries.

‡ Electron microscopic section taken from edge of necrosis.

TABLE II

RESULTS WITH PROTON AND ALPHA-PARTICLE IRRADIATION USING DOSES BETWEEN 6.7 AND 7.7 KRAD AND LARGE-BLOCK RECOVERY METHOD FOR PREPARATION OF TISSUES

								Microscopic findings						
								Light microscopy			Electron microscopy †			
*Rabbit No.**	*Area Tissue studied*	*Dose (krad)*	*Energy (mev)*	*Aperture diam. (in.)*	*Age at irrad. (days)*	*Days aft. irrad. at sacrifice*	*Gross les.*	*Hemorrhage*	*Gliosis*	*Demyelination*	*Capil. basal lamina thick ‡*	*Incr. fibrils in foot processes*	*Endothel. swell.*	*Capil. stasis*
5	Irrad.	7.0	910	⅜	75	57	—	—	—	—	—	—	—	—
	Near les.						+				200/5	++	+	+
	Free of les.						—	+	++	++	100/3	+	+	ō
	Control	ō	—	—	—	—	ō	ō	ō	ō	85/11	++	ō	ō
6	Irrad.	7.0	910	⅜	75	61	—	—	—	—	—	—	—	—
	Near les.						+				267/3	++	+++	++
	Free of les.						—	+	++	++	116/6	++	++	+
	Control	ō	—	—	—	—	ō	ō	ō	ō	86/3	+	ō	ō
7	Irrad.	7.0	910	⅜	75	61	—	—	—	—	—	—	—	—
	Near les.						+				166/3	+++	++	+
	Free of les.						—	++	++	++	90/2	+	ō	ō
	Control	ō	—	—	—	—	ō	ō	ō	ō	96/3	++	ō	ō
8	Irrad.	6.8	38	¼	64	88	+	ō	+	+	166/3	NE	++	+
	Control	ō	—	—	—	—	ō	ō	ō	ō	90/2	ō	ō	ō
9	Irrad.	7.6	40	¼	59	225	ō	ō	ō	ō	NE	NE	NE	NE
	Control	ō	—	—	—	—	ō	ō	ō	ō	NE	NE	NE	NE

* Brain tissue of Rabbits 5, 6, and 7 was irradiated with alpha-particle radiation; that of Rabbits 8 and 9, with proton radiation.

† NE, not examined.

‡ Expressed as average thickness in millimicrons per number of measurements on different capillaries.

TABLE III

RESULTS WITH PROTON IRRADIATION USING DOSES BETWEEN 6.0 AND 6.5 KRAD AND AN APERTURE OF ONE-FOURTH IN.

Rabbit No.	*Area tissue studied*	*Dose (krad)*	*Energy (mev)*	*Age at irrad. (days)*	*Days aft. irrad. at sacrifice*	*Gross les.*	*Microscopic findings **					
							Light microscopy			*Electron microscopy*		
							Hemorrhage	*Gliosis*	*Demyelination*	*Capil. basal lamina thick.†*	*Incr. fibrils in foot processes*	*Endothel. swell.*	*Capil. stasis*
10	Irrad.	6.4	42	56	24	ō	ō	ō	ō	175/2	++	+	+
	Control	ō	—	—	—	ō	ō	ō	ō	NE	NE	NE	NE
11	Irrad.	6.2	42	56	28	ō	ō	ō	ō	91/7	ō	ō	ō
	Control	ō	—	—	—	ō	ō	ō	ō	NE	NE	NE	NE
12‡	Irrad.	6.0	37.5	84	33	ō	++	++	++	76/3	++	+++	++
	Control	ō	—	—	—	ō	ō	ō	ō	85/4	ō	ō	ō
13§	Irrad.	6.2	42	56	67	ō	ō	+++	++	90/7	++	++	++
	Control	ō	—	—	—	ō	ō	+	ō	NE	NE	NE	NE
14‖	Irrad.	6.1	37.5	84	69	ō	NE	NE	NE	97/7	++	+	+
	Control	ō	—	—	—	ō	ō	ō	ō	66/5	ō	ō	+
15¶	Irrad.	6.3	37.5	86	69	ō	NE	NE	NE	70/3	++	++	++
	Control	ō	—	—	—	ō	ō	ō	ō	67/6	ō	+	+

* NE, not examined.

†Expressed as average thickness in millimicrons per number of measurements on different capillaries.

‡ Same animal as Rabbit 1, but opposite side of brain.

§ Same animal as Rabbit 2, but opposite side of brain.

‖ Same animal as Rabbit 4, but opposite side of brain.

¶ Same animal as Rabbit 3, but opposite side of brain.

TABLE IV

RESULTS WITH ALPHA-PARTICLE IRRADIATION USING A DOSE OF 5.5 KRAD AND 910 MEV

Rabbit No.	Area tissue studied	Aperture diam. (in.)	Age at irrad. (days)	Days aft. irrad. at sacrifice	Gross lesion	Microscopic findings: Light microscopy: Hemorrhage	Light microscopy: Gliosis	Light microscopy: Demyelination	Electron microscopy *: Capil. basal lamina thick.†	Electron microscopy *: Incr. fibrils in foot processes	Electron microscopy *: Endothel. swell.	Electron microscopy *: Capil. stasis
16	Irrad.	¼	75	47	ō	ō	ō	ō	47/9	ō	ō	ō
	Control	—	—	—	ō	ō	ō	ō	52/4	++	+	ō
17	Irrad.	¼	75	47	ō	++	+++‡	++	150/6	++	ō	ō
	Control	—	—	—	ō	ō	ō	ō	93/3	ō	ō	ō
18	Irrad.	¼	75	53	ō	ō	+	ō	66/3	++	ō	ō
	Control	—	—	—	ō	ō	+	ō	55/4	++	ō	ō
19	Irrad.	¼	75	61	ō	ō	ō	ō	51/4	++	ō	ō
	Control	—	—	—	ō	ō	ō	ō	65/4	+	ō	ō
20	Irrad.	⅜	63	69	ō	ō	ō	ō	200/1	+++	+	ō
	Control	—	—	—	ō	ō	ō	ō	66/3	ō	ō	ō
21	Irrad.	⅜	63	69	ō	+	ō	ō	40/3	+	ō	ō
	Control	—	—	—	ō	ō	ō	ō	NE	NE	NE	NE
22	Irrad.	¼	75	76	ō	++§	+++	+	48/4	++	ō	ō
	Control	—	—	—	ō	ō	+	ō	50/3	+	ō	ō
23	Irrad.	⅜	63	97	ō	+	ō	ō	75/6	+	+	ō
	Control	—	—	—	ō	+	ō	ō	65/5	+	+	ō

* NE, not examined.

† Expressed as average thickness in millimicrons per number of measurements on different capillaries.

‡ Microscopic area of necrosis 0.5 mm. in diameter in white matter.

§ Areas of frank tissue necrosis.

TABLE V

RESULTS WITH PROTON IRRADIATION USING DOSES BETWEEN 2.4 AND 5.49 KRAD

Rabbit No.	Area tissue studied	Dose (krad)	Energy (mev)	Aperture diam. (in.)	Age at irrad. (days)	Days aft. irrad. at sacrifice	Gross les.	Microscopic findings: Light microscopy: Hemorrhage	Light microscopy: Gliosis	Light microscopy: Demyelination	Electron microscopy *: Capil. basal lamina thick.†	Electron microscopy *: Incr. fibrils in foot processes	Electron microscopy *: Endothel. swell.	Electron microscopy *: Capil. stasis
24	Irrad.	5.4	47.5	¼	56	12	ō	ō	ō	ō	95.8	++	+	ō
	Control	ō	—	—	—	—	ō	ō	ō	ō	80/4	+	+	—
25‡	Irrad.	5.3	40	¼	57	225	+	ō	++	+	416/3	++	+	ō
	Control	ō	—	—	—	—	ō	ō	ō	ō	62/2	+	ō	ō
26	Irrad.	2.5	37.5	⅛	86	196	+	++	++	+	NE	NE	NE	NE
	Control	ō	—	—	—	—	ō	ō	ō	ō	NE	NE	NE	NE

* NE, not examined.

† Expressed as average thickness in millimicrons per number of measurements on different capillaries.

‡ The large-block recovery method was used in preparing tissue from Rabbit 25 for examination.

band of reactive astrocytes along its edges. At lower radiation doses producing delayed radionecrosis (Table II), the typical lesion as seen in the light microscope consists of a central area of gitter cells or occasionally a spongy neuropil with a few recognizable cells will remain. Sclerosed blood vessels are often recognizable in and about these areas. Perivascular hemorrhages are sometimes observed, usually separate from any area of distinct necrosis. White matter tends to be more involved than does gray matter. Demyelination is seen about areas of necrosis and perivascular hemorrhage. About the edges of areas of frank necrosis, gliosis is often intense. In those instances in which frank necrosis has not yet occurred, there may be some increase in the glial cells and fibrils, but this is not usually marked. Where there is no frank necrosis and gliosis, there is no vessel sclerosis. Accumulations of amyloid-like material are only occasionally found.

Electron-microscopic examination of areas within the radiation field, but not showing necrosis by gross examination, shows swelling of the endothelial cells and thickening of capillary basal lamina; e.g., 110 mμ versus 90 mμ (the term "basal lamina," as proposed by Fawcett,[20] is used rather than "basement membrane," which has a less restricted meaning in light microscopy). An increase in glial fibrils, both in astrocytic foot processes and at sites removed from the capillary wall, is also seen. In addition, there are increased numbers of irregularly shaped and irregularly staining inclusions and vacuoles in the astrocytic foot processes.

In material taken directly for osmification from the glutaraldehyde-perfused brain, one is never sure that the tissue being examined in the electron microscope is not in or adjacent to an area of necrosis, and the changes observed in capillaries might therefore be secondary to the necrosis rather than related to the development of necrosis. In tissue from Rabbits 5, 6, and 7, in the study of which the large-block recovery method was used (Table II), however, it is possible to exclude any nearby necrosis by preliminary light microscopy (Fig. 2) over the entire 1-cm. square section. In those tissues in which the large-block recovery method was used, 3 areas were taken for electron microscopy. These areas were: tissue adjacent to areas showing early radionecrosis (Fig. 3); the tissue in the beam path but showing no relationship to areas of radiation necrosis by light microscopy (Fig. 4); and the control tissue out of the beam path taken from the boundary between the gray and white matter (Fig. 5). Areas adjacent to early radiation necrosis were characterized by capillary basal lamina thickening (Text-fig. 1), excrescences of the basal lamina and morphologic changes in the cytoplasm of endothelial cells and pericytes (Fig. 3). These changes consisted of an increase in multivesicular bodies and in number and size of

vacuoles, a decrease in endoplasmic reticulum and ribosomes, and loss of general staining of the background cytoplasm. The extracellular space appeared to be increased, and glial processes adjacent to the capillary basal lamina had increased number of dark inclusions and electron-dense banding of the plasma membrane adjacent to the basal lamina.

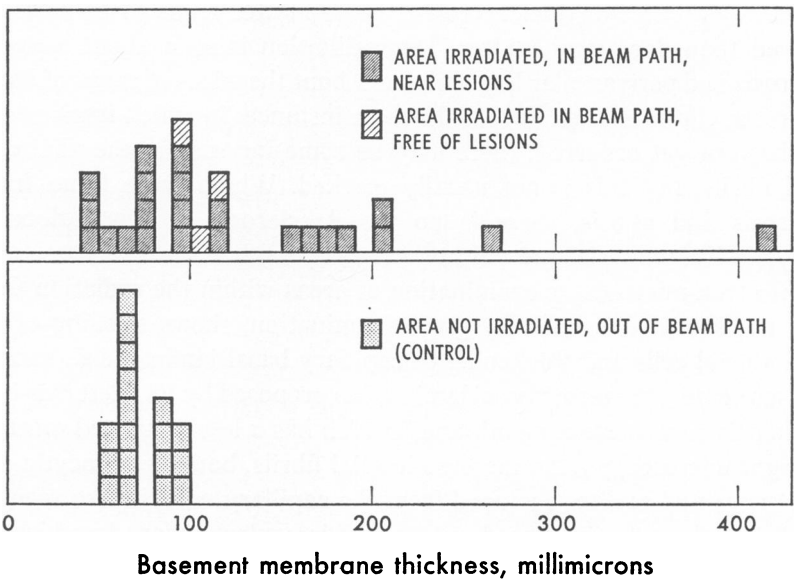

TEXT-FIG. 1. Distribution of basal lamina thickness (averages from Table 1–5) of control and irradiated areas of brains of 22 animals. Blocks with narrow diagonals indicate area irradiated in beam path, near lesions (in Tables, "irradiated"—without mention of relationship to lesions). Blocks with wide diagonals, area irradiated in beam path, free of lesions; determined by large-block recovery method. Blocks with stippling, control (not irradiated, out of beam path) and from left cerebrum of glass-bead injected animal. Average basal lamina thickness, 100 mμ.

Tissue in the beam path, but showing no relationship to areas of necrosis, also showed capillary basal lamina thickening but to a lesser degree (Text-fig. 1). The morphologic changes in endothelial cells and pericytes described above were also found in this tissue but were not generally as advanced as in the case of tissue adjacent to necrotic areas. In Fig. 4, however, the changes are shown to be quite advanced, with marked vacuolation of the endothelial cell cytoplasm at the left of the field. There is irregular splitting of the basal lamina running diagonally across the field, and many irregular inclusions are present in the pericyte cytoplasm in the upper right of the field.

Scanning electron microscopy produced stereoscopic information about the structure of capillaries of hemorrhagic (Fig. 6) and control (Fig. 7) areas of the brain. The depth of the section (4 μ) can be seen,

and the inside of the capillary wall, the more rigid basal lamina at the crest of the wall, red blood cells, and the surrounding neuropil are all shown in three-dimensional aspect. The basal lamina appears much thinner in the control region (Fig. 7) than in the hemorrhagic area (Fig. 6), supporting the results of the measurement done by standard two-dimensional electron microscopy (Text-fig. 1).

The necrotic areas produced by the injection of the 14–40-μ glass beads were found more often in white matter than in gray matter. Irregular inclusions, vacuoles, and apparently degenerating mitochondria are present in the astrocyte cytoplasm, and prominent electron-dense "beading" is apparent where glial fibrils meet the cytoplasmic membrane adjacent to the basal lamina. The basal lamina itself is often split or broken although the endothelial cytoplasm may appear normal near necrotic areas produced by glass-bead injection.

Discussion

From the results presented, there is no doubt that thickening of capillary basal lamina occurs following particle radiation of the rabbit brain. Similar findings have been reported by Cervós-Navarro[21] using ^{60}Co gamma radiation. Even before the large-block recovery method was developed, it was thought that this thickening of the basal lamina precedes or occurs independent of necrosis. Using the large-block recovery method it was found that capillaries distant from areas of necrotic tissue but in the beam path show basal lamina thickening but less than that seen near areas of necrotic tissue; basal lamina splitting and apparently autolytic changes in the cytoplasm of all cellular components adjacent to the capillary are seen in these irradiated areas not related to necrotic tissue. Similar capillary changes have been described in chronic turpentine abscesses in muscle.[22]

Capillary alterations appear to precede general tissue necrosis. The fact that there are fewer capillaries in white matter[23] would explain necrosis occurring selectively here where the failure of 1 capillary makes up a higher percentage of the total capillary supply than where more capillaries are present as in gray matter.

In the scanning electron micrographs there is increased prominence of the basal lamina in the irradiated area with perivascular hemorrhage (Fig. 6 and 7). The prominence of the basal lamina is due both to its thickness and its height above the adjacent section surface. It appears that the basal lamina has more rigidity than other tissue components that are retracted down to form a lower level of the sectioned surface. In nonirradiated areas, the entire capillary basal lamina and endothelium is thinner than in the irradiated area. With the scanning electron micro-

scope one has a stereoscopic image of surfaces with the additional advantage of continuous magnification from less than × 50 (for surveying 1-sq. cm. tissue sections) to an effective magnification of more than × 5000 (with a resolution of better than 0.1 μ). With newer instruments of this type becoming available, resolution should be better than 200 Å.

Following glass-bead injection, the necrotic foci involve white matter more than gray matter. Astrogliosis is present but generally less marked than in the radiation-induced lesions. Also sclerosis of vessels in the lesion is not a feature as in the case of the radiation-induced lesion. The electron micrographs show some splitting of basal lamina of capillaries, but the basal lamina is less thickened and without surface irregularities. Interestingly, one sees beads of increased electron density where glial fibrils (microtubules) come in contact with plasma membrane adjacent to the basal lamina. The plasma membrane is indistinct in these areas. Similar changes are seen in the plasma membrane in irradiated brains (Fig. 3 and 8). One is tempted to conjecture that these changes in glial fibrils are related to alterations in the transfer of metabolites by the glial cells. With aldehyde fixation such microtubules as glial fibrils are being shown to interconnect many of the membrane systems of the cell. Sandborn[24] has demonstrated connections between microtubules and other membrane structures, such as mitochondria, endoplasmic reticulum, and plasma membrane. He believes these microtubules may serve a transport function within the cell, as well as providing mechanical support function within the cell or as a means of mechanical motion as has been the usual interpretation.

Using a fourfold chi-square test with the Yates small-number correction, the thickening of the capillary basal lamina is significant to $p<0.01$. There is considerable overlap of measurements of both irradiated and control areas, but more important is the lack of any control measurements greater than 100 mμ (Text-fig. 1). Our experience with localization of cyclotron beams makes us confident that the control tissue lay outside of the beam path and did not receive more than 1% of the radiation dose. However, without any gross or microscopic lesions in the beam path, there is always the possibility that the "irradiated" tissue taken for electron microscopy was not in the beam path. Thus it is to be expected that some "irradiated" capillary basal lamina measurements would fall in the control range because, in fact, the tissue was not irradiated. The control areas, however, were never irradiated and never have capillary basal lamina thicknesses in the radiated range (greater than 100mμ).

While the present study strongly supports the hypothesis that capillary alterations are the primary cause of radionecrosis, certain observa-

tions suggesting primary effects on glial cells should be noted. Studies of Zeman[7] showed disturbances of nucleic acid metabolism of glial cells preceding delayed radionecrosis, and the morphologic observations of Baily[6] demonstrated differential radiosensitivity of cells in chronic lesions. Alteration in capillary structure, as shown in the present paper, appears to be sufficient to interfere both with passage of blood through the lumens and with maintenance of permeability of the capillary wall. Changes in nucleic acid metabolism and in morphology of the glial cells could occur secondarily to capillary failure and subsequent tissue injury.[25] The primary effects of central nervous system irradiation leading to delayed necrosis appear to be associated with the capillary bed.

Conclusions and Summary

Increase in capillary basal lamina thickness is regularly seen from 1 to 3 months following proton or alpha-particle irradiation of the rabbit brain. This thickening is present in areas adjacent to radionecrotic tissue.

Radiation changes that appear in areas not related to necrotic tissue include endothelial- and perivascular-cell edema. The number and size of cytoplasmic vacuoles and inclusions is increased. Splitting of capillary basal lamina is present, but thickening of basal lamina is not so marked as in areas adjacent to necrotic tissue.

The scanning electron microscope and a large-block recovery method for transmission electron microscopy were used to show that the capillary changes are limited to the irradiated area and that capillary basal lamina thickening is found primarily in areas adjacent to necrotic tissue.

References

1. Lindgren, M. On tolerance of brain tissue and sensitivity of brain tumors to irradiation. *Acta Radiol 170*(Supp.):1–73, 1958.
2. Boellaard, J. W., and Jacoby, W. Roentgenspätschäden des Gehirns. *Acta Neurochir (Wien) 10:*533–566, 1962.
3. Dynes, J. B., and Smedal, M. I. Radiation myelitis. *Amer J Roentgen 83:*78–87, 1960.
4. Scholz, W. Über die Empfindlichkeit des Gehirns für Röntgen- und Radiumstrahlen. *Klin Wschr 14:*189–193, 1935.
5. Russell, D. S., Wilson, C. W., and Tansley, K. Experimental radio-necrosis of the brain in rabbits. *J Neurol Neurosurg Psychiat 12:*187–195, 1949.
6. Bailey, O. T., Woodard, J. S., and Putnam, T. J. "Tissue Reactions of the Human Frontal White Matter to Gamma Radiation." In *Response of Nervous System to Ionizing Radiation,* Haley, T. J., and Snider, R. S. Eds. Little, Boston, 1964, pp. 3–18.
7. Zeman, W. Disturbances of nucleic acid metabolism preceding delayed radionecrosis of nervous tissue. *Proc Nat Acad Sci USA 50:*626–630, 1963.
8. Lawrence, J. H., Tobias, C. A., Born, J. L., Wang, C. C., and Linfoot, J. H. Heavy-particle irradiation in neoplastic and neurologic disease. *J Neurosurg 19:*717–722, 1962.

9. TOBIAS, C. A., ANGER, H. O., and LAWRENCE, J. H. Radiological use of high energy deuterons and alpha particles. *Amer J Roentgen 67:*1–27, 1952.
10. LARSSON, B., LEKSELL, L., and REXED, B. The use of high energy protons for cerebral surgery in man. *Acta Chir Scand 125:*1–7, 1963.
11. BIRGE, A. C., ANGER, H. O., and TOBIAS, C. A. "Heavy Charged-Particle Beams." In *Radiation Dosimetry,* HINE, G. J., and BROWNELL, G. L., Eds. Acad. Press, New York, 1965, pp. 623–665.
12. PALAY, S. L., MCGEE-RUSSELL, S. M., GORDON, S., JR., and GRILLO, M. A. Fixation of neural tissues for electron microscopy by perfusion with solutions of osmium tetroxide. *J Cell Biol 12:*385–410, 1962.
13. GLAUERT, A. M., and GLAUERT, R. H. Araldite as an embedding medium for electron microscopy. *J Biophys Biochem Cytol 4:*191–194, 1958.
14. LUFT, J. H. Improvements in epoxy resin embedding methods. *J Biophys Biochem Cytol 9:*409–414, 1961.
15. REYNOLDS, E. S. The use of lead citrate at high pH as an electron-opaque stain in electron microscopy. *J Cell Biol 17:*208–212, 1963.
16. GRIMLEY, P. M. Selection for electron microscopy of specific areas in large epoxy tissue sections. *Stain Technol 40:*259–263, 1965.
17. DE BRUIJN, W. C., and MCGEE-RUSSELL, S. M. Bridging a gap in pathology and histology. *J Roy Microscop Soc 85:*77–90, 1966.
18. OATLEY, C. W., NIXON, W. C., and PEASE, R.F.W. Scanning electron microscopy. *Advances Electron Electron Phys 21:*181–247, 1965.
19. MCDONALD, L. W., PEASE, R.F.W., and HAYES, T. L. Scanning electron microscopy of sectioned tissue. *Lab Invest 14:*13–18, 1967.
20. FAWCETT, D. W. *The Cell, Its Organelles and Inclusions: An Atlas of Fine Structure.* Saunders, Philadelphia, 1966, p. 353.
21. CERVÓS-NAVARRO, J. Elektronenmikroskopische Befunde an den Capillaren des Kaninchengehirns nach der Einwirkung ionisierender Strahlen. *Arch Psychiat Nervenkr 205:*204–222, 1964.
22. FUCHS, U. Die Ultrastruktur der Blutcapillaren bei einer chronischen Entzündung. *Frankfurt Z Path 74:*544–554, 1965.
23. COBB, S. "The Cerebrospinal Blood Vessels." In *Cytology and Cellular Pathology of the Nervous System* (Vol. 2), PENFIELD, W., Ed. Hafner, New York, 1965, pp. 577–610.
24. SANDBORN, E., SZEBERENYI, A., MESSIER, P. E., and BOIS, P. A new membrane model derived from a study of filaments, microtubules and membranes. *Rev Canad Biol 24:*243–276, 1965.
25. KONIGSMARK, B. W., and SIDMAN, R. L. Origin of brain macrophages in the mouse. *J Neuropath Exp Neurol 22:*643–676, 1963.

The authors wish to thank Dr. R. F. W. Pease, Department of Electrical Engineering, for his help and advice in using the scanning electron microscope. The construction of the microscope was largely supported by the United States Air Force Avionics Laboratory and by the University of California Electronics Research Laboratory.

Thanks are also due Mrs. Frances Taylor for technical help in preparing ultrathin sections; Mr. Michael P. Donovan and Mrs. Winifred M. Palmer for their help in preparing the large sections of the epoxy-embedded tissue, using the Jung microtome; and to the crews of the 88-in. cyclotron and the 184-in. cyclotron used in the irradiation of the animals.

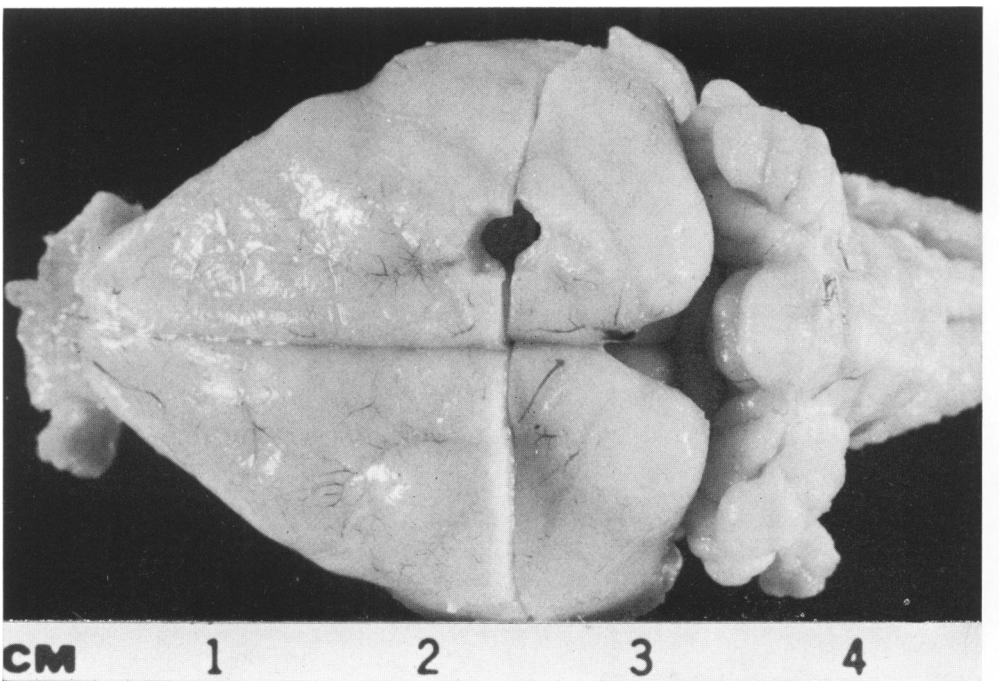

FIG. 1. Brain (Rabbit 3) with radiation-induced hole in sensory cortex of right lobe of cerebrum. Dose was 25 krad, using 0.3-cm. diameter, 37.5-mev proton beam; animal was sacrificed 69 days following irradiation.

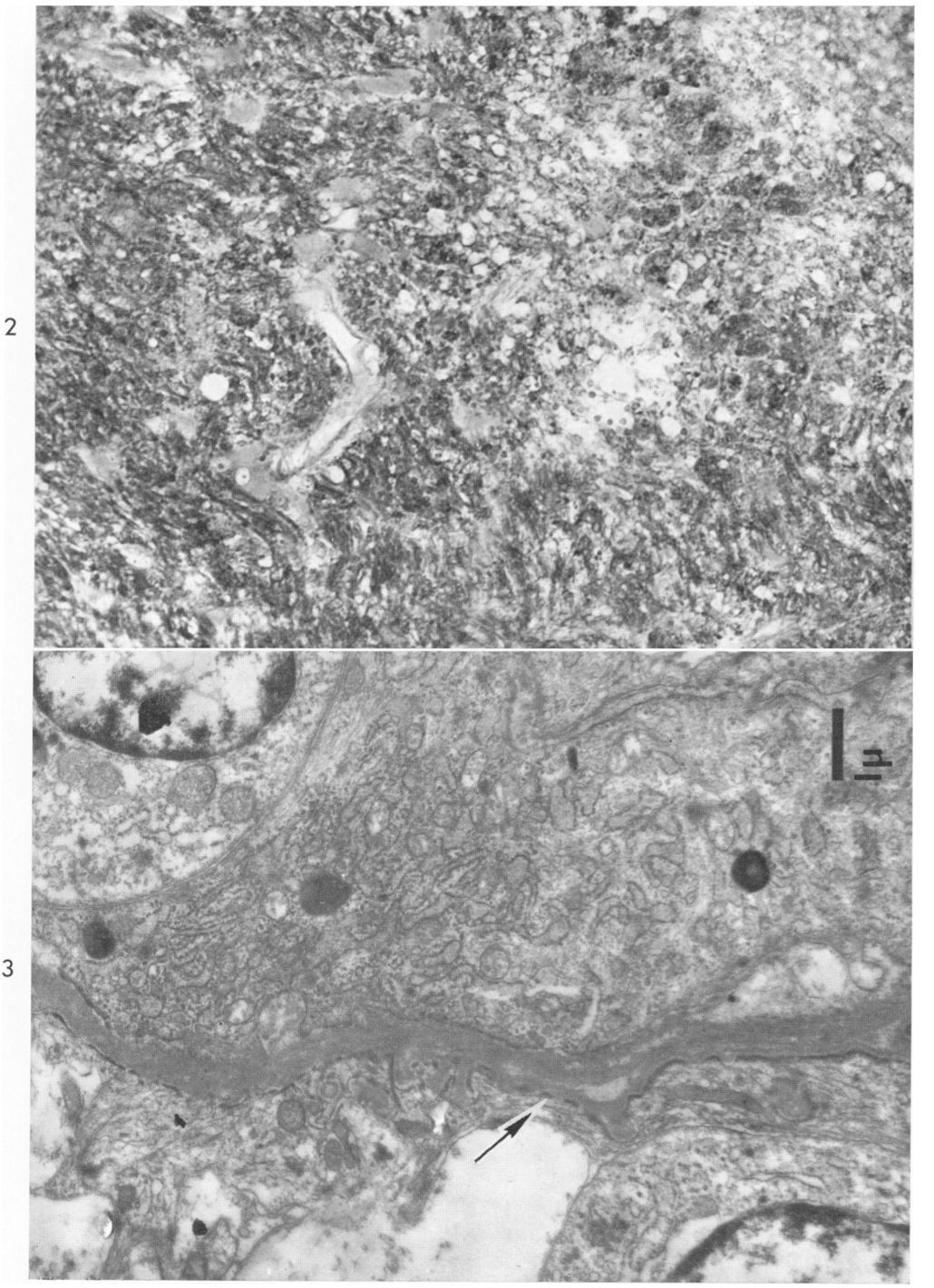

FIG. 2. Brain tissue, 8-μ thick section (Rabbit 6). Material obtained by large-block recovery method. Small areas of necrotic tissue at right of center, with ghost outlines of tissue components remaining. Giemsa stain. × 250.

FIG. 3. Areas of increased electron density where glial fibrils meet plasma membrane (arrow) cross field adjacent to thickened capillary basal lamina.

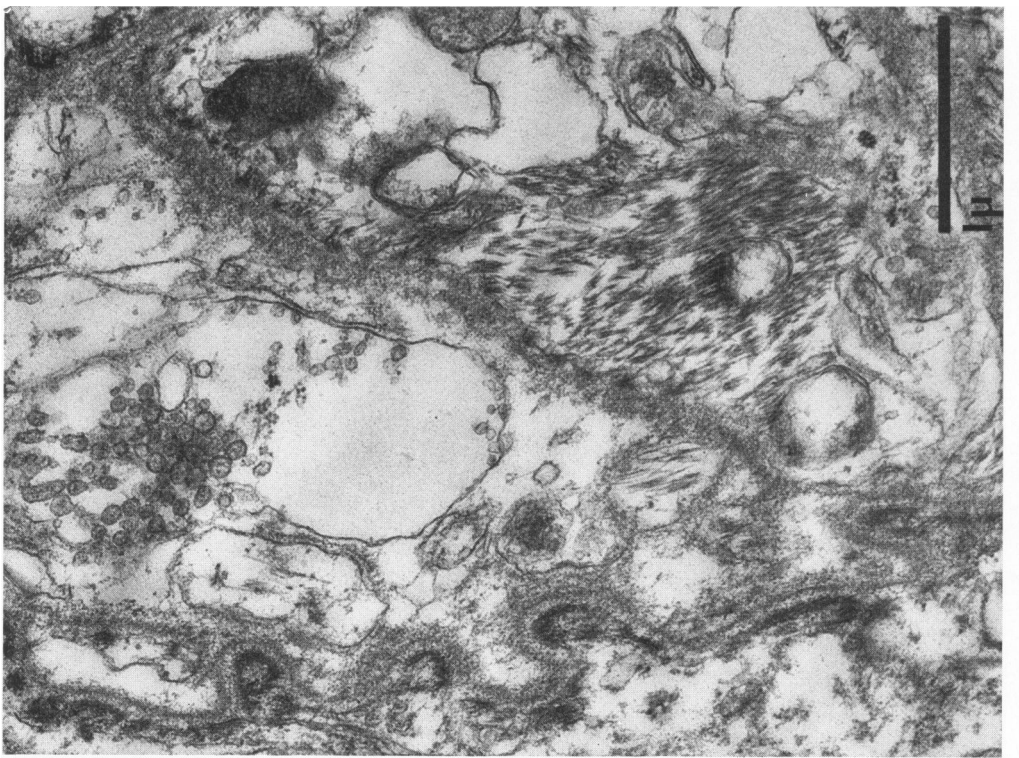

4

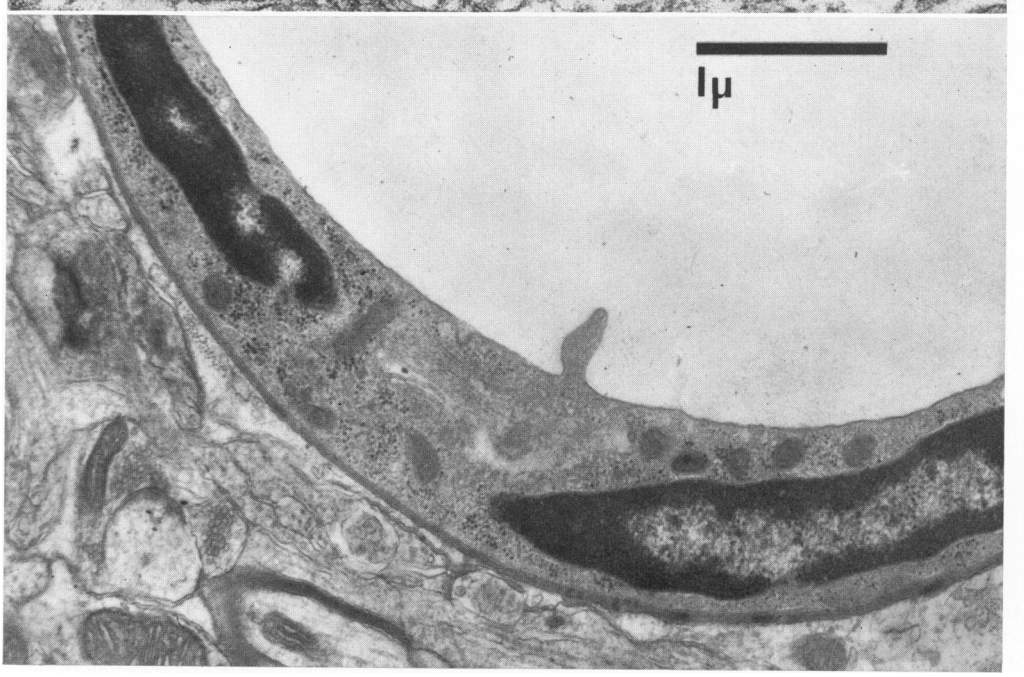

5

FIG. 4. Tissue from same block (Fig. 2), within beam path but removed from radionecrosis, shows splitting of capillary basal lamina, edema of pericyte and endothelial-cell cytoplasm, and increased numbers of various inclusions. × 28,000.

FIG. 5. Capillary outside radiation field (same tissue block as Fig. 2). × 25,000.

FIG. 6. Scanning-beam electron micrograph using secondary electron mode. Tissue is from area of perivascular hemorrhage (Rabbit 7). Red cells appear in three-dimensional aspect within blood vessel at top. Prominent basal lamina stands out at edge of vessel (arrow). Part of capillary is present across lumen (double arrow), where glass supporting section is seen as dark background. × 5000; 45° specimen tilt.

FIG. 7. Scanning electron micrograph taken outside beam path shows capillary wall cut longitudinally (Rabbit 7). Inside wall of capillary at bottom, neuropil at top. × 5000; 45° specimen tilt.

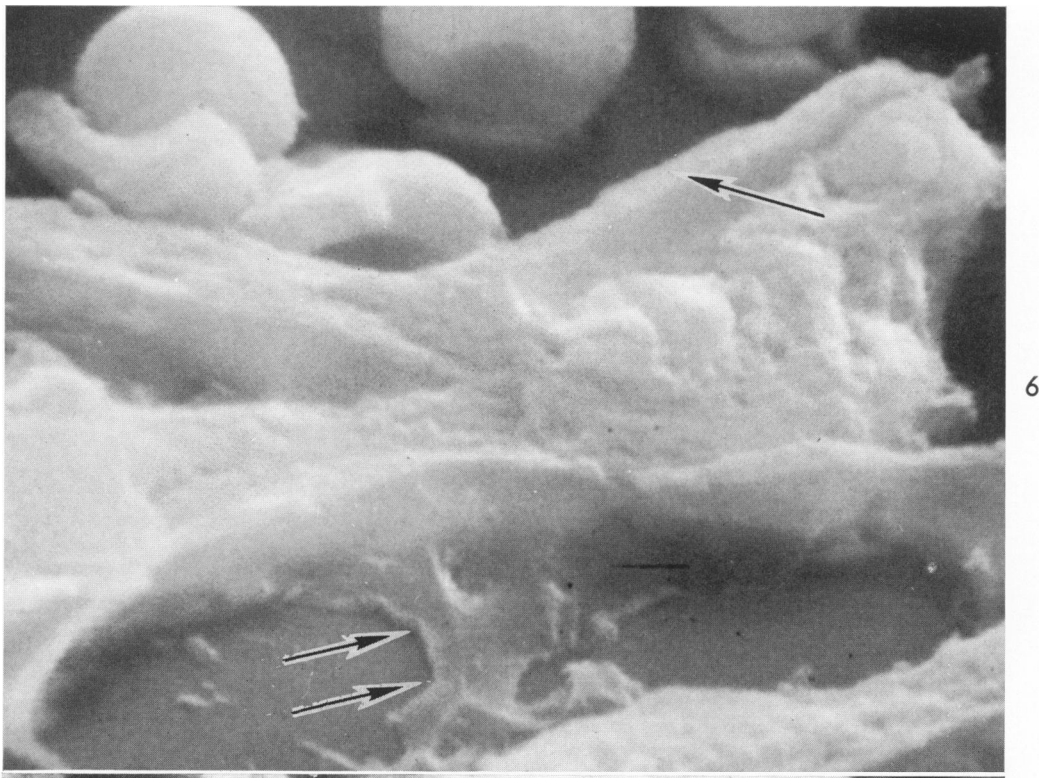

6

7

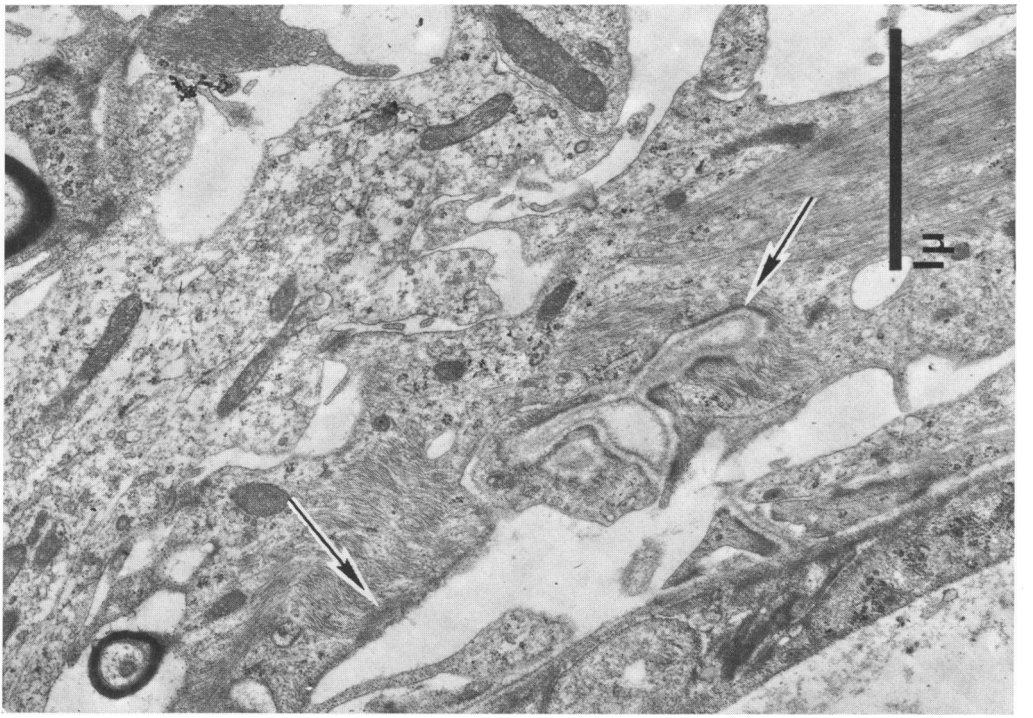

FIG. 8. Electron-dense banding (Rabbit 5) where glial fibrils meet plasma membrane (arrows). Capillary lumen at lower right. 7.0 krad near lesion. × 31,000.